Combustion and Flame 162 (2015) 2693–2704

Contents lists available at ScienceDirect

Combustion and Flame

journal homepage: www.elsevier.com/locate/combustflame

High-temperature chemistry of HCl and Cl_2

Matteo Pelucchi [a], Alessio Frassoldati [a], Tiziano Faravelli [a,*], Branko Ruscic [b,c], Peter Glarborg [d]

[a] Dipartimento di Chimica, Materiali e Ingegneria Chimica "G. Natta", Politecnico di Milano, P.zza Leonardo da Vinci 32, 20133 Milano, Italy
[b] Chemical Sciences and Engineering Division, Argonne National Laboratory, Argonne, IL 60439, USA
[c] Computation Institute, University of Chicago, Chicago, IL 60637, USA
[d] DTU Chemical Engineering, Technical University of Denmark, 2800 Lyngby, Denmark

ARTICLE INFO

Article history:
Received 23 February 2015
Received in revised form 2 April 2015
Accepted 3 April 2015
Available online 22 April 2015

Keywords:
Chlorine
Hydrogen chloride
Kinetics
Oxidation
Flame inhibition

ABSTRACT

The high temperature chlorine chemistry was updated and the inhibition mechanisms involving HCl and Cl_2 were re-examined. The thermochemistry was obtained using the Active Thermochemical Tables (ATcT) approach, resulting in improved data for chlorine-containing species of interest. The HCl/Cl_2 chemistry discussed in the paper was based on reference and experimental measurements of rate constants available in the literature. By coupling the new HCl/Cl_2 subset with the Politecnico di Milano (POLIMI) syngas mechanism a kinetic mechanism consisting of 25 species and 102 reactions was obtained. The validation was carried out on selected experimental data from laminar flames, shock tubes and plug flow reactors. Systems containing Cl_2 showed high sensitivity to $Cl_2 + M \rightleftharpoons Cl + Cl + M$; the rate constant for this reaction has a significant uncertainty and there is a need for an accurate high-temperature determination. The importance of the chain propagating steps such as $Cl + H_2 \rightleftharpoons HCl + H$ and $Cl_2 + H \rightleftharpoons HCl + Cl$ competing with the branching reaction $H + O_2 \rightleftharpoons OH + O$ and the termination reaction $H + Cl + M \rightleftharpoons HCl + M$ is also pointed out by the kinetic analysis. Other relevant reactions in HCl containing systems are the chain propagation reactions $HCl + O \rightleftharpoons Cl + OH$, $HCl + OH \rightleftharpoons Cl + H_2O$ and $Cl + HO_2 \rightleftharpoons ClO + OH$, together with the termination reaction $Cl + HO_2 \rightleftharpoons HCl + O_2$. With the present thermochemistry and rate constants, reaction cycles involving HOCl and ClCO were found not to be important under the investigated conditions.

© 2015 The Combustion Institute. Published by Elsevier Inc. All rights reserved.

1. Introduction

The chlorine chemistry in combustion and gasification of solid fuels is a concern, partly due to the possibility of pollutant emissions and partly due to the corrosive potential of chlorine. In particular annual biomass and certain waste fractions may contain chlorine in significant quantities [1]. Chlorine is typically released during pyrolysis as chlorinated hydrocarbons (e.g., chloromethane, CH_3Cl), hydrogen chloride (HCl) or alkali chloride (mainly KCl). During combustion the chlorine will largely be oxidized and emitted as HCl. Hydrogen chloride is typically the desired chlorine containing product in combustion, because it can easily be removed from the flue gas by a scrubbing process. However, chlorine is known to participate also in dioxin/furan formation through mechanisms that may involve high-temperature gas phase reactions as well as low-temperature reactions catalyzed by fly ash [2–4].

The presence of chlorine may affect the overall combustion process as well as the fate of other pollutants [1]. Chlorine species is known to inhibit fuel oxidation [5–9], even though the effect is less pronounced than for other halogens such as bromine [10]. The content of chlorine in a fuel may also have an impact on NO_x-emissions [11] and on the formation of PAH and soot [12,13]. In addition, chlorine may affect the partitioning of trace metals such as Cd, Cu, Mn, Zn, Cr, As, Hg, and lead salts [14,15]. In particular the effect of chlorine on mercury speciation has received attention [16–18]. Other examples include interaction between chlorine and potassium in biomass combustion, leading to formation of aerosols and/or corrosive deposits [19–23].

A high chlorine content in a fuel may act to inhibit ignition [24], lower flame speeds [25], and facilitate flame quenching [26]. The presence of HCl [5,6,8] or chlorinated hydrocarbons [7,9,27] is also known to inhibit oxidation of CO to CO_2 under reactor conditions. The interaction of HCl with the O/H radical pool is quite complex, and even though the overall mechanism of inhibition is known [1,6], details are still under investigation. Presumably, the inhibition takes place through simple cycles, initiated by chain propagating steps such as

$$HCl + H \rightleftharpoons Cl + H_2 \quad \text{(R2b)}$$

* Corresponding author.

http://dx.doi.org/10.1016/j.combustflame.2015.04.002
0010-2180/© 2015 The Combustion Institute. Published by Elsevier Inc. All rights reserved.

$$HCl + OH \rightleftharpoons Cl + H_2O \quad (R4)$$

and completed by terminating reactions like

$$Cl + H + M \rightleftharpoons HCl + M \quad (R1)$$

$$Cl + HO_2 \rightleftharpoons HCl + O_2 \quad (R6)$$

As the Cl atom concentration builds up in the post flame region, reactions (R2) and (R4) may become partially equilibrated and even driven in the reverse direction. Under these conditions inhibition is significantly reduced [6]. The inhibiting cycles compete with a chain propagating cycle [28],

$$Cl + HO_2 \rightleftharpoons ClO + OH \quad (R7)$$

$$ClO + CO \rightleftharpoons Cl + CO_2 \quad (R48)$$

which corresponds to the overall reaction $CO + HO_2 \rightarrow CO_2 + OH$. The competition between these cycles determines whether the chlorine has an overall promoting or inhibiting effect on the fuel oxidation. The inhibition process is sensitive to the branching ratio of the $Cl + HO_2$ reaction, which is well established only at low temperatures [29].

Evaluations of the elementary reactions involved in chlorine chemistry at combustion conditions have been reported by Baulch et al. [30] and more recently by Senkan [31]. Kinetic modeling studies have mostly focused on chloromethane [9,25,32,33], but also studies of chlorine inhibition of CO oxidation in flow reactors [5] and in flames [34] have been reported.

Despite the considerable interest in high-temperature chlorine reactions, details of the chemistry remain uncertain. The thermodynamic properties of oxygenated chlorine species have been in question and most chlorine reactions have only been characterized experimentally at low temperatures, if at all. Furthermore, no reported chlorine reaction mechanisms have been validated over a wider range of conditions. The objective of the present work is to update our knowledge of the high-temperature chlorine chemistry, emphasizing reactions of HCl and Cl_2 deserving investigation or better assessment. The thermochemistry of the chlorine species is re-examined and the hydrogen/chlorine/oxygen reaction mechanism is updated. The resulting model is validated against selected experimental data from literature and used to analyze the effect of HCl and Cl_2 on laminar, premixed hydrogen and syngas flames.

2. Thermochemistry

The thermochemistry of the chlorine-containing species of interest, given in Table 1, was obtained using the Active Thermochemical Tables (ATcT) approach [35,36], which, in contrast to the traditional "sequential" approach, derives accurate, reliable, and internally consistent thermochemical values by analyzing and simultaneously solving [37–40] the underlying Thermochemical Network (TN). A TN is constructed from the available thermochemical interdependencies relevant to the targeted species, such as measured reaction enthalpies, bond dissociation energies, constants of equilibria, ionization energies, electron affinities, etc. [41,42]. One of the advantages of the ATcT TN is that it allows commingling of experimental and computational results, the latter typically obtained from state-of-the-art electronic structure methods. The most recent previous version of the ATcT TN [40], has been updated to accommodate, inter alia, the targeted chlorine-containing species. Overall, the current ATcT TN (ver. 1.122) [43] contains over 1180 chemical species of interest to combustion and atmospheric chemistry, interconnected by more than 19,000 determinations.

ATcT outputs, in form of tables of enthalpies of formation, heat capacities, entropies, and enthalpy increments, covering the range 298–6000 K, were fitted to 7-term polynomials using the NASA program of McBride and Gordon [44]. Table 1 lists the current ATcT thermochemistry for the chlorine-containing species of interest. The respective NASA polynomials are given in the Supplementary Material. Note that Table 1 lists the values as obtained directly from the current version of ATcT. The polynomials, which are subject to inherent fitting errors because of the 7-term limitation, produce very slightly different values.

3. Reaction mechanism

The chemical kinetic model used in the present study consists of a H_2/CO oxidation scheme together with a subset for the Cl/H/O system. The H_2/CO oxidation mechanism was adopted from the work by Frassoldati et al. [45] and by Cuoci et al. [46] and has been validated over a broad range of conditions. The complete mechanism is available in Chemkin format with thermo and transport properties on the CreckModeling web site (http://creckmodeling.chem.polimi.it), and also reported as Supplementary Material to this paper.

The chlorine subset of the reaction mechanism is listed in Table 2. The key steps in the H_2/Cl_2 system, i.e.,

$$H + Cl + M \rightleftharpoons HCl + M \quad (R1)$$

$$Cl + H_2 \rightleftharpoons HCl + H \quad (R2)$$

$$Cl + Cl + M \rightleftharpoons Cl_2 + M \quad (R9)$$

$$H + Cl_2 \rightleftharpoons HCl + Cl, \quad (R10)$$

are among the few chlorine reactions that have been characterized over a wider temperature range. The thermal dissociation of HCl (R1b) has been measured at high temperatures in shock tube studies [47,73–77]. The early work was evaluated by Baulch et al. [30] who made a recommendation for k_{1b} for the temperature range

Table 1
Thermodynamic properties for selected chlorine species. Units are kcal mol^{-1} and cal mol^{-1} K^{-1}.

Species	$H_{f,0}$	$H_{f,298}$	±	S_{298}	$C_{p,300}$	$C_{p,400}$	$C_{p,500}$	$C_{p,600}$	$C_{p,800}$	$C_{p,1000}$	$C_{p,1500}$	$C_{p,2000}$
HCl	−21.986	22.030	0.001	44.670	6.964	6.973	7.004	7.069	7.289	7.562	8.149	8.529
Cl_2	0.000	0.000	exact	53.317	8.122	8.436	8.620	8.735	8.870	8.949	9.073	9.194
Cl	28.590	28.992	0.000	39.482	5.223	5.370	5.436	5.445	5.389	5.314	5.175	5.101
ClO	24.169	24.311	0.008	53.800	8.243	8.436	8.587	8.699	8.847	8.941	9.094	9.217
HOCl	−17.655	−18.357	0.006	56.540	8.926	9.580	10.113	10.529	11.140	11.602	12.423	12.918
OClO	24.146	23.556	0.069	61.395	10.058	11.011	11.745	12.282	12.963	13.356	13.849	14.103
ClOO	24.814	24.552	0.086	65.759	11.329	11.811	12.206	12.527	12.979	13.256	13.589	13.723
ClCHO	−42.927	−43.693	0.217	61.919	10.707	12.067	13.210	14.155	15.591	16.599	18.052	18.746
ClCO	−5.242	−4.908	0.114	63.154	10.682	11.233	11.645	11.989	12.524	12.891	13.382	13.595
HOOCl	0.923	−0.339	0.231	64.070	12.694	14.033	14.975	15.658	16.589	17.227	18.242	18.805
ClOOCl	32.148	31.375	0.130	70.995	15.733	17.134	17.965	18.481	19.049	19.332	19.626	19.733

Table 2
Rate coefficients for reactions in the Cl/H/O subset of the reaction mechanism. The rate constants are expressed in terms of a modified Arrhenius expression, $K = A\,T^{n}\,\exp(-E_a/(RT))$. Units are cm, mol, s, cal.

		A	n	E_a	$\Delta H_{rxn,\,298}$	Source
1.	$H + Cl + M \rightleftharpoons HCl + M$[a]	2.0E23	−2.450	0	−103.1	[47][b]
2.	$Cl + H_2 \rightleftharpoons HCl + H$	9.5E07	1.720	3060	1.1	[85]
3.	$HCl + O \rightleftharpoons Cl + OH$	5.9E05	2.114	4024	0.4	[49]
4.	$HCl + OH \rightleftharpoons Cl + H_2O$	4.1E05	2.120	−1284	−15.7	[50]
5.	$Cl + H_2O_2 \rightleftharpoons HCl + HO_2$	6.6E12	0.000	1950	−15.5	[51]
6.	$Cl + HO_2 \rightleftharpoons HCl + O_2$	7.5E14	−0.630	0	−54.0	See text
7.	$Cl + HO_2 \rightleftharpoons ClO + OH$	3.8E13	0.000	1133	1.2	[51]
8.	$Cl + O_3 \rightleftharpoons ClO + O_2$	1.5E13	0.000	417	−36.2	[30]
9.	$Cl + Cl + M \rightleftharpoons Cl_2 + M$[c]	2.3E19	−1.500	0	−58.6	See text
10.	$Cl_2 + H \rightleftharpoons HCl + Cl$	8.6E13	0.000	1172	−45.1	[30]
11.	$Cl_2 + O \rightleftharpoons Cl + ClO$	4.5E12	0.000	3279	−6.3	[52]
12.	$Cl_2 + OH \rightleftharpoons HOCl + Cl$	2.2E08	1.350	1480	1.7	[53]
13.	$Cl + OH + M \rightleftharpoons HOCl + M$	1.2E19	−1.430	0	−56.3	[33][b]
14.	$HOCl \rightleftharpoons ClO + H$	8.1E14	−2.090	93690	94.8	[33]
15.	$HOCl + H \rightleftharpoons HCl + OH$	6.1E07	1.960	421	−46.8	[54]
16.	$HOCl + H \rightleftharpoons ClO + H_2$	4.4E−4	4.890	425	−9.4	[55]
17.	$HOCl + O \rightleftharpoons ClO + OH$	3.3E03	2.900	1592	−7.9	[54]
18.	$HOCl + OH \rightleftharpoons ClO + H_2O$	1.3E00	3.610	−2684	−24.1	[54]
19.	$HOCl + HO_2 \rightleftharpoons ClO + H_2O_2$	8.8E−7	5.350	6978	7.4	[54]
20.	$HOCl + Cl \rightleftharpoons HCl + ClO$	3.5E−1	4.070	−337	−8.3	[55]
21.	$ClO + H \rightleftharpoons Cl + OH$	3.8E13	0.000	0	−38.5	[56]
22.	$ClO + H \rightleftharpoons HCl + O$	8.4E12	0.000	0	−38.9	[56]
23.	$ClO + O \rightleftharpoons Cl + O_2$	1.5E13	0.000	−219	−54.9	[51]
24.	$ClO + OH \rightleftharpoons HCl + O_2$	3.5E05	1.670	−3827	−55.3	[57]
25.	$ClO + HO_2 \rightleftharpoons HOCl + O_2$	7.8E03	2.370	5111	−45.6	[57][d]
		8.4E02	2.260	−449		
26.	$ClO + HO_2 \rightleftharpoons HCl + O_3$	4.6E03	2.050	1699	−17.8	[57]
27.	$ClO + HO_2 \rightleftharpoons ClOO + OH$	4.6E05	1.800	2116	6.3	[57]
28.	$ClO + HO_2 \rightleftharpoons OClO + OH$	1.3E03	2.320	5099	5.3	[57]
29.	$ClO + ClO \rightleftharpoons Cl_2 + O_2$	6.6E10	0.660	3759	−48.6	[57]
30.	$ClO + ClO \rightleftharpoons Cl + ClOO$	8.2E10	0.770	4308	4.9	[57]
31.	$ClO + ClO \rightleftharpoons Cl + OClO$	3.8E13	0.005	5754	3.9	[57]
32.	$ClO + O(+M) \rightleftharpoons OClO(+M)$	2.6E13	−0.030	−85	−60.3	[58]
	Low pressure limit	3.1E27	−4.10	835		
33.	$OClO(+M) \rightleftharpoons Cl + O_2(+M)$	1.1E16	−0.280	58756	5.4	[58]
	Low pressure limit	9.9E−24	11.00	33100		
34.	$OClO + H \rightleftharpoons ClO + OH$	4.7E13	0.000	0	−42.4	[59]
35.	$OClO + O \rightleftharpoons ClO + O_2$	5.2E07	1.450	876	−58.8	[60]
36.	$OClO + OH \rightleftharpoons HOCl + O_2$	3.3E04	2.070	−4102	−50.9	[61]
37.	$OClO + ClO \rightleftharpoons ClOO + ClO$	6.0E01	2.800	155	1.0	[62]
38.	$Cl + O_2(+M) \rightleftharpoons ClOO(+M)$	1.0E14	0.000	0	−4.5	[58]
	Low pressure limit	6.0E28	−5.34	1341		
39.	$ClOO + H \rightleftharpoons ClO + OH$	3.4E13	0.000	0	−43.4	[30]
40.	$ClOO + O \rightleftharpoons ClO + O_2$	1.5E12	0.000	1910	−59.8	[51]
41.	$ClOO + OH \rightleftharpoons HOCl + O_2$	2.0E12	0.000	0	−51.9	est
42.	$ClOO + Cl \rightleftharpoons Cl_2 + O_2$	1.3E14	0.000	0	−53.5	[63]
43.	$CH_2O + Cl \rightleftharpoons HCO + HCl$	4.9E13	0.000	68	−12.9	[64]
44.	$CH_2O + ClO \rightleftharpoons HCO + HOCl$	7.2E10	0.790	5961	−4.6	[65]
45.	$HCO + Cl \rightleftharpoons HCl + CO$	1.0E14	0.000	0	−87.4	[34] est
46.	$HCO + Cl_2 \rightleftharpoons ClCHO + Cl$	3.8E12	0.000	72	−25.1	[66]
47.	$HCO + ClO \rightleftharpoons HOCl + CO$	3.2E13	0.000	0	−79.1	[6]
48.	$CO + ClO \rightleftharpoons CO_2 + Cl$	2.4E05	2.020	10500	−62.9	[67]
49.	$ClCHO + M \rightleftharpoons HCl + CO + M$	5.0E15	0.000	40000	−4.7	[68], est
50.	$ClCHO + H \rightleftharpoons ClCO + H_2$	9.9E05	2.250	3861	−13.3	[69]
51.	$ClCHO + H \rightleftharpoons HCO + HCl$	1.1E06	2.120	6905	−20.4	[69]
52.	$ClCHO + O \rightleftharpoons ClCO + OH$	4.2E11	0.570	2760	−11.9	est
53.	$ClCHO + OH \rightleftharpoons ClCO + H_2O$	2.2E13	0.000	2822	−28.0	[70]
54.	$ClCHO + Cl \rightleftharpoons ClCO + HCl$	7.2E12	0.000	1620	−12.2	[64]
55.	$Cl + CO + M \rightleftharpoons ClCO + M$	1.2E24	−3.800	0	−7.5	[51]
56.	$ClCO + H \rightleftharpoons CO + HCl$	1.0E14	0.000	0	−95.6	[71]
57.	$ClCO + O \rightleftharpoons CO + ClO$	1.0E14	0.000	0	−56.8	[34] est
58.	$ClCO + O \rightleftharpoons CO_2 + Cl$	1.0E14	0.000	0	−119.7	[34] est
59.	$ClCO + OH \rightleftharpoons CO + HOCl$	3.3E12	0.000	0	−48.8	[71]
60.	$ClCO + O_2 \rightleftharpoons CO_2 + ClO$	7.9E10	0.000	3300	−64.8	[6]
61.	$ClCO + Cl \rightleftharpoons CO + Cl_2$	6.6E13	0.000	1400	−50.5	[72]

[a] Third body efficiencies: $H_2 = 2$, $Cl_2 = 2$, $N_2 = 2$, $H_2O = 5$.
[b] Calculated from the reverse rate constant and the equilibrium constant.
[c] Third body efficiencies: $H_2 = 2$, $Cl_2 = 6.9$, $N_2 = 2$, $H_2O = 5$
[d] Duplicate reaction; the rate constant is calculated by adding the two Arrhenius expressions.

2900–7000 K. In the present work, we rely on the more recent shock tube determination of Schading and Roth [47], who extended the temperature range down to 2500 K. Their measured value of k_{1b} agrees within 50% in the overlapping temperature range with the previous studies. The rate constants for (R1b) proposed by Baulch et al. and by Schading and Roth do not extrapolate well down to low temperatures where the reverse reaction, recombination of H and Cl atoms, may become important. For this reason, we choose to describe the rate of reaction in terms of k_1 with an AT^{β} expression, derived from the Schading and Roth data and microscopic reversibility.

The reaction between HCl and H (R2b) is almost thermo-neutral. It has been measured over a broad temperature range both in the forward [78–81] and reverse [48,79,80,82–85] direction, but only Adu and Fontijn [81,48] and Lee et al. [83] have obtained data at temperatures higher than 500 K. Theory [86,87] is in reasonable agreement with the experimental results. Figure 1 shows an Arrhenius plot for Cl + H_2 (R2). We have adopted the rate constant proposed by Kumaran et al. [85] that provides a good representation of the available measurements.

Reaction (R10), H + Cl_2, is fast. It has been characterized at temperatures up to 730 K. Reported activation energies for (R10) vary between 500 and 1800 cal mol^{-1}. We have adopted the recommendation of Baulch et al. [30], which is based on measurements by Wagner et al. [88] and Bemand and Clyne [89]. The Baulch rate constant is supported by the more recent work by Berho et al. [90].

The recombination of atomic Cl to form Cl_2 has been measured at low temperature in the forward direction (R9) and at high temperature in shock tubes in the reverse direction (R9b). The results were evaluated by Lloyd [91] and Baulch et al. [30]. The high temperature data fall in three groups. The early measurements of Hiraoka and Hardwick [92] and Diesen and Felmlee [93] indicate values of k_{9b} an order of magnitude higher than the bulk of the data. The high values have been attributed to boundary layer effects and limitations in detection accuracy and were disregarded by both Lloyd [91] and Baulch et al. [30]. The data from Jacobs and Giedt [94], van Thiel et al. [95], and Carabetta and Palmer [96] are in good agreement and these data form the basis for the recommendation of Lloyd [91]. The third group of data, reported by Blauer et al. [97] and Santoro et al. [98], indicate a rate constant for Cl + Cl + Ar that is about a factor of five below the bulk data. Baulch et al. chose to disregard most of the high temperature results for Cl_2 dissociation, claiming that high levels of Cl_2 made it difficult to separate the effects of Ar and Cl_2 as collision partners, and based their evaluation on the results of Blauer et al. [97].

Predicted flame speeds and ignition delays for Cl_2/H_2 mixtures are sensitive to the choice of k_9, as discussed below. These results indicate a dissociation rate for Cl_2 that is higher than that proposed by Baulch et al. [30] and perhaps even faster than the recommendation of Lloyd. Our proposed rate constant, in an AT^{β} format (Fig. 2) is in reasonable agreement with the high-temperature recommendation of Lloyd (converted to values for the Cl + Cl recombination through the equilibrium constant) and with the most reliable data for k_9 [99–104]. The shock tube results for (R9b) are consistent with a collision efficiency of Cl_2 about 6.9 times higher than that of Ar [30]; the low temperature data for (R9) indicate a slightly lower value.

The rate constant proposed in the current work is seen to be well below the value used by Leylegian et al. [105] in their recent study of Cl_2/H_2 flame speeds (Fig. 2). The rate constant from Leylegian et al. is compatible with the early shock tube determinations from Hiraoka and Hardwick [92] and Diesen and Felmlee [93] but it is contradicted by a fairly substantial body of data from more recent studies. More work is desirable on this important reaction.

Reactions of HCl with oxygen-containing radicals include

$$HCl + O \rightleftharpoons Cl + OH \quad (R3)$$

$$HCl + OH \rightleftharpoons Cl + H_2O \quad (R4)$$

$$HCl + HO_2 \rightleftharpoons Cl + H_2O_2 \quad (R5b)$$

The HCl + O reaction has been measured over a wide temperature range. The theoretical study by Xie et al. [49] offers a rate constant in good agreement with the recommendation of Baulch et al. [30], as well as more recent studies by Mahmoud et al. [106] and Hsiao et al. [107]. The only discrepancy occurs at temperatures above 2000 K where the data from Hsiao et al. indicate a change in curvature in the Arrhenius plot that is not confirmed by the theoretical study. The reaction of HCl with OH has been studied extensively, but only the studies of Hack et al. [108], Husain et al. [109], Ravishankara et al. [110], and Bryukov et al. [50] present data

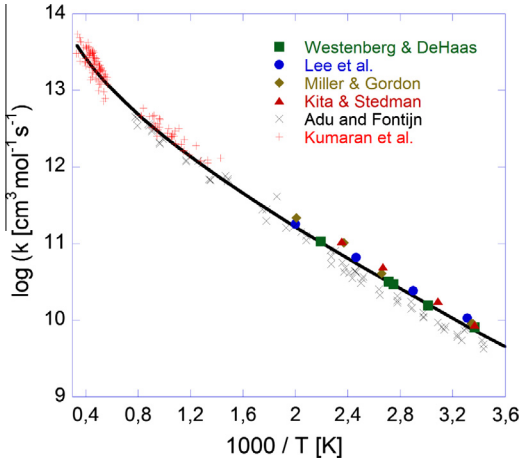

Fig. 1. Arrhenius plot for the reaction Cl + H_2. Experimental results (symbols) from Westenberg and DeHaas [82], Lee et al. [83], Miller and Gordon [79], Kita and Stedman [80], Kumaran et al. [85], Adu and Fontijn [48]. The solid line denotes the rate constant recommended by Kumaran et al.

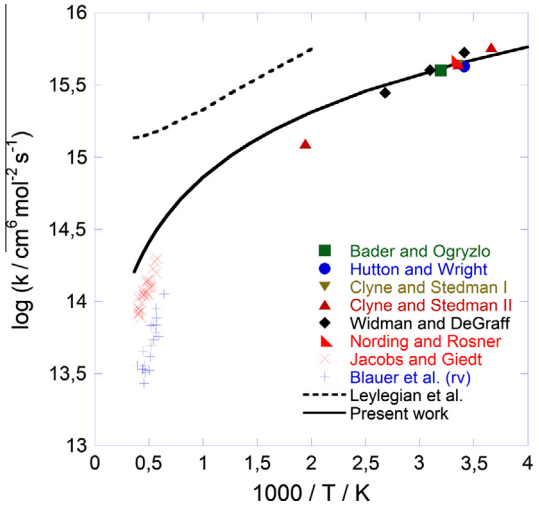

Fig. 2. Arrhenius plot for the reaction Cl + Cl + M. Experimental results (symbols) from Bader and Ogryzlo [99], Hutton and Wright [100], Clyne and Stedman [101,102], Widman and DeGraff [103], Nording and Rosner [104], Jacobs and Giedt [94], and Blauer et al. [97]. The data from Jacobs and Giedt and from Blauer et al. were obtained for the reverse reaction and converted through the equilibrium constant in the present work. The solid line represents the preferred rate constant in the present work, while the dashed line represents the recommendation of Leylegian et al. [105].

obtained above 500 K. There is some scatter at higher temperatures, but the results of Bryukov et al. are in agreement with most data within the combined uncertainties. The $HCl + HO_2$ reaction has not been studied experimentally, but there are low temperature data for the reverse step,

$$Cl + H_2O_2 \rightleftharpoons HCl + HO_2 \quad (R5)$$

The data are quite scattered and the only results above room temperature, from Michael et al. [111] and Keyser [112], do not extend beyond 500 K. Following Atkinson et al. [51], we have adopted the rate constant from Keyser, but the uncertainty at elevated temperatures is significant.

The reaction between atomic Cl and HO_2 has two product channels, an exothermic, chain terminating step,

$$Cl + HO_2 \rightleftharpoons HCl + O_2 \quad (R6)$$

and a thermo-neutral, chain propagating step

$$Cl + HO_2 \rightleftharpoons ClO + OH \quad (R7)$$

The competition between these two channels has a significant impact on the inhibition of fuel oxidation by chlorine species. The overall rate constant and the branching fraction between the two channels have only been measured at low temperature. Atkinson et al. [51] based their recommendations of k_6 and k_7 on results of the direct studies of Lee and Howard [113], Riffault et al. [114] and Hickson and Keyser [29], which are in good agreement (230–420 K). The extrapolation to higher temperatures is uncertain. Gavriliv et al. [115] reported a rate constant for the $HCl + O_2$ reaction (R6b) of 5×10^{12} exp(-26000/T) $cm^3\,mol^{-1}\,s^{-1}$ for the temperature range 853–1423 K. From the equilibrium constant, we have converted their measurements to values of k_6 and used these data for extrapolation of the low temperature values of k_6 (Fig. 3).

Reactions of molecular chlorine with O and OH lead to formation of oxygenated chlorine species:

$$Cl_2 + O \rightleftharpoons ClO + Cl \quad (R11)$$

$$Cl_2 + OH \rightleftharpoons HOCl + Cl \quad (R12)$$

For (R11) we rely on the measurement of Wine et al. [52], which appears to have less interference from secondary reactions than the earlier work reviewed by Baulch et al. [30], while for reaction (R12) we adopt the rate constant determined by Bryukov et al. [53].

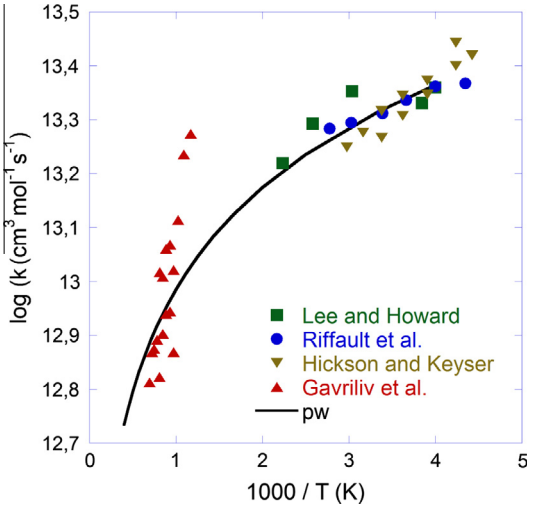

Fig. 3. Arrhenius plot for the reaction $Cl + HO_2$. Experimental results (symbols) from Lee and Howard [113], Riffault et al. [114], Hickson and Keyser [29], and Gavriliv et al. [115]. The data from Gavriliv et al., obtained for the reverse reaction, were converted in the present work. The solid line represent a best fit to the experimental data.

HOCl may dissociate thermally,

$$HOCl + M \rightleftharpoons Cl + OH + M \quad (R13b)$$

or react with the radical pool,

$$HOCl + H \rightleftharpoons HCl + OH \quad (R15)$$

$$HOCl + H \rightleftharpoons ClO + H_2 \quad (R16)$$

$$HOCl + O \rightleftharpoons ClO + OH \quad (R17)$$

$$HOCl + OH \rightleftharpoons ClO + H_2O \quad (R18)$$

$$HOCl + HO_2 \rightleftharpoons ClO + H_2O_2 \quad (R19)$$

$$HOCl + Cl \rightleftharpoons HCl + ClO \quad (R20)$$

No experimental data have been reported for (R13b); we use a rate constant for the Cl + OH + M recombination (R13) based on the QRRK calculation of Ho et al. [33]. The reactions of HOCl with radicals are all exothermic, except for (R19). For reactions (R15), (R17), (R18) and (R19), for which there are no reported measurements at higher temperatures, the calculated rate constants from Xu and Lin [54] have been adopted. Their values for k_{15} and k_{18} are in good agreement with available experimental data [116,117], while their rate constant for (R17) disagrees with the low temperature measurements by Schindler et al. [118]. The value of k_{20} was drawn from Wang et al. [55].

The ClO radical reacts rapidly with the radical pool,

$$ClO + H \rightleftharpoons Cl + OH \quad (R21)$$

$$ClO + H \rightleftharpoons HCl + O \quad (R22)$$

$$ClO + O \rightleftharpoons Cl + O_2 \quad (R23)$$

$$ClO + OH \rightleftharpoons Cl + HO_2 \quad (R7b)$$

$$ClO + OH \rightleftharpoons HCl + O_2 \quad (R24)$$

$$ClO + HO_2 \rightleftharpoons HOCl + O_2 \quad (R25)$$

Similarly to HOCl, reactions of ClO have only been studied at low temperatures. However, they are mostly quite exothermic and would not be expected to have a strong temperature dependency. For the ClO + H reactions (R21, R22), we rely on the room temperature measurements from Wategaonkar and Setser [56], while for ClO + O (R23) we follow the recommendation of Atkinson et al. [51]. The reactions of ClO with OH (R7b, R24) and HO_2 (R25–R28) were studied theoretically by Zhu and Lin [57]. For ClO + OH, the calculated rate constants agree well with the low temperature measurements of the total rate constant and branching fraction [119–121]. However, with the present thermodynamic data, the low temperature measurements of the forward and reverse rate constants for $ClO + OH \rightleftharpoons Cl + HO_2$ (R7b) are not internally consistent and more work is required to solve this discrepancy. The $ClO + HO_2$ reaction has several product channels, including H-abstraction to form $HOCl + O_2$ (R25). The Zhu and Lin rate constants are compatible with measurements of the overall rate constant, e.g., [122,123].

Subsets for the isomers ClOO and OClO were included in the reaction mechanism. Rate constants were drawn from low temperature measurements [30,51,59,63] and from theoretical work by Lin and coworkers [58,60–62]. However, these species are not significant under the conditions of the present work due to their low thermal stability.

Experimental results on inhibition of H_2 oxidation by HCl and Cl_2 are very limited, but data have been reported on inhibition of moist CO oxidation in flames and flow reactors [5,6,8,124]. For this reason, a subset was established describing the interactions of CH_xO with chlorine species (R43-R61). Oxidation of CO to CO_2 may be facilitated by reactions with chlorine species, either directly,

$$ClO + CO \rightleftharpoons Cl + CO_2 \quad (R48)$$

or through the sequence,

$$Cl + CO + M \rightleftharpoons ClCO + M \quad (R55)$$

$$ClCO + O_2 \rightleftharpoons ClO + CO_2 \quad (R60)$$

Louis et al. [67] calculated the rate constant for (R48) from ab initio theory. Their value is well below the upper limit at 587 K reported by Clyne and Watson [125], but an experimental verification is desirable. For (R55) we have adopted the recommendation of Atkinson et al. [51], which is based on the low-temperature measurements of Nicovich et al. [126] and agrees well with the relative rate measurements from Hewitt et al. [127]. The rest of the ClCO subset, including the exothermic reaction with O_2 (R60), was drawn from the mechanism of Roesler et al. [5]. The rate constants for these steps are rough estimates and involve a considerable uncertainty. Also a subset for ClCHO was included in the model, but this component is formed in negligible amounts under the investigated conditions.

Reactions of ozone may conceivably play a role in chain termination at low temperatures for chlorine/O_2 systems. For this reason, we include an O_3 reaction subset with rate constants from Atkinson et al. [128]. Also the reaction

$$Cl + O_3 \rightleftharpoons ClO + O_2 \quad (R10)$$

is included in the mechanism. It is of interest in atmospheric chemistry and has been studied extensively at low temperature. The recommendation of Baulch et al. [30] represents well these data and extrapolates reasonably well to the results of Park [129] at 950–1350 K, the only study reported at elevated temperature.

4. Results and discussion

Earlier experimental results on the H_2/Cl_2 system include explosion limits H_2/Cl_2 [130,131], laminar flame speeds [105], flame structure [132], and shock tube results [133]. Studies on the inhibition of moist CO oxidation by HCl in flow reactors [5,6,8] and chlorine inhibition in flames [124] were also presented. The following section discusses a detailed comparison of experimental data with model simulations. All simulations were performed with the OpenSMOKE code [134,135] using the kinetic scheme described above. Computed sensitivity coefficient, S_y, was normalized (s_y) as follows:

$$s_y = \frac{\delta \ln y}{\delta \ln A} = \frac{A \delta y}{y \delta A} = \frac{A}{y} S_y$$

where y is the model variable (species concentration, temperature) and A the generic frequency factor of the rate constant expressed in the usual Arrhenius form, $k = A\,T^{\beta}\exp(-E_A/(RT))$.

4.1. Shock tube ignition delays for H_2/Cl_2 mixtures

Ignition delay times of H_2/Cl_2 in argon were measured in a 2 inches internal diameter shock tube by Lifshitz and Schechner [133] over the temperature range 830–1260 K. The ignition time was defined as the time interval between the arrival of the reflected shock and the ignition point, identified by a steep rise in pressure or, correspondingly, in the heat flux. The condition after the reflected shock was determined from the incident shock velocity. Compositions, initial (P_1) and reflected pressures (P_5) of the tested mixtures are reported in Table 3. The measured ignition delay times were accurately correlated through the following relation,

$$\tau_{ign} = 10^{-12.73}\exp(18750/RT)[Cl_2]^{-0.66}[H_2]^{-0.60}[Ar]^{0.40}\ [s]$$

Here the concentrations are in mol cm^{-3} and the apparent activation energy is in cal mol^{-1}.

Figure 4 compares calculated and experimental ignition delay times. Although the model is able to accurately reproduce both the effect of increasing pressure, for instance when comparing induction times of mixture A with mixture B, and varying reactant concentrations (A versus D or A versus C), it is up to a factor of 2 slower than the experimental values for T < 1000 K.

To better investigate the chemistry involved in the ignition of H_2/Cl_2 mixtures, sensitivity analyses have been carried out at different temperatures, pressures and mixture compositions. Results are shown in Fig. 5. The reactivity of the system is largely controlled by the chain initiation reaction $Cl_2 + M \rightleftharpoons Cl + Cl + M$ (R9b) and by the chain propagation reaction $Cl + H_2 \rightleftharpoons HCl + H$ (R2), forming the highly reactive H atom. While the sensitivity coefficients are not strongly influenced by pressure, a larger variation is observed for increasing temperatures and for increasing Cl_2 concentrations (mixture A versus mixture D).

Figure 6 shows the effect on the modeling predictions for mixture B of using the rate constant proposed by Leylegian et al. [105], which is significantly above our preferred value. The use of the larger value of k_9 improves modeling predictions, with a 30% reduction of the calculated ignition delay times. However, both sets of calculations are considered to be in fairly good agreement with the experimental data, except at the lowest temperatures where boundary effects are known to be more pronounced.

Table 3
Experimental conditions of ignition delay time measurements for H_2/Cl_2 mixtures [133].

Mixture	H_2 (mol%)	Cl_2 (mol%)	P_1 (atm)	P_5 (atm)
A	10.4	10.4	0.066	1.0
B	10.4	10.4	0.263	4.6
C	19.8	10.0	0.066	1.3
D	10.3	21.6	0.066	1.3
E	11.0	11.0	0.066	1.3

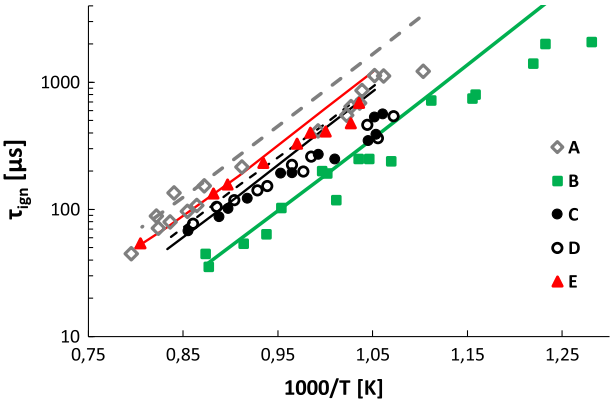

Fig. 4. Comparison between experimental measurements [133] and calculated ignition delay times for $H_2/Cl_2/Ar$ mixtures. The composition of mixtures A, B, C, D, and E is reported in Table 3.

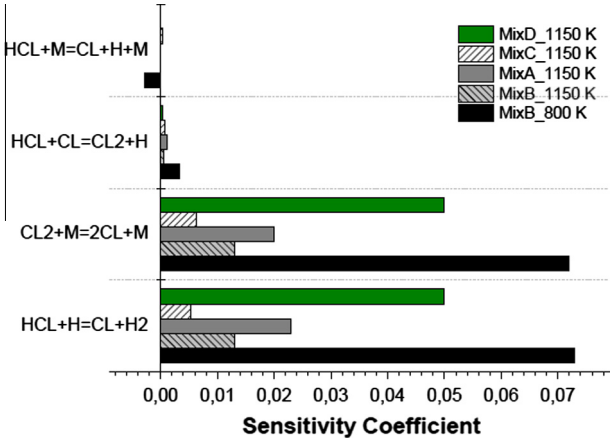

Fig. 5. Sensitivity coefficients of ignition delay times to rate constants for $H_2/Cl_2/Ar$ mixtures at different temperatures, pressures and compositions.

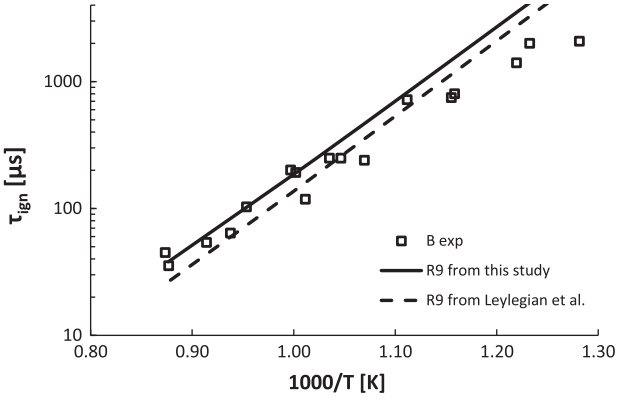

Fig. 6. Effect of including the rate constant adopted by Leylegian et al. [105] for R9b on ignition delay times (Mixture B [133]); shown as the dashed line.

4.2. Laminar flame speed of $H_2/Cl_2/N_2$ mixtures

The laminar flame speeds of H_2/Cl_2 mixtures were measured by Leylegian et al. [105] using the counterflow twin-flame technique. Reactants were diluted in nitrogen at mole fractions of 0.50, 0.55 and 0.60 to limit the laminar flame speed to the range of 15–50 cm s^{-1}. Estimated uncertainties are in the order of 1–2 cm s^{-1}. Measured and calculated laminar flame speeds are reported in Fig. 7 as a function of the equivalence ratio. The equivalence ratio ϕ is defined as the ratio H_2/Cl_2 in the mixture, assumed the unit value for the stoichiometric mixture (H_2:Cl_2 = 1:1). Model predictions are found to be in reasonable agreement with experimental data particularly for 0.55 and 0.6 nitrogen dilution, while for N_2 = 0.5 and equivalence ratios higher than 1.4 the mechanism strongly underestimates the laminar flame speed. Similar deviations between experimental results and modeling predictions were observed by Leylegian et al. [105].

In an attempt to explain these deviations, sensitivity analyses were carried out for ϕ = 1.0 (N_2 = 0.5 and 0.6), 1.6 and 2.0 (N_2 = 0.5). Results are reported in Fig. 8. The flame propagation is largely dominated by the chain initiation reaction (R9b) and the chain propagation (R2), similarly to what we previously observed for ignition delay times calculation. Lower sensitivity coefficients are calculated for the chain propagation reaction R10 enhancing reactivity and for the termination reaction R1, inhibiting flame propagation particularly for high equivalence ratios (increasing H_2/decreasing Cl_2 concentrations in the mixture). It is also evident from Fig. 8 that sensitivity coefficients do not change significantly

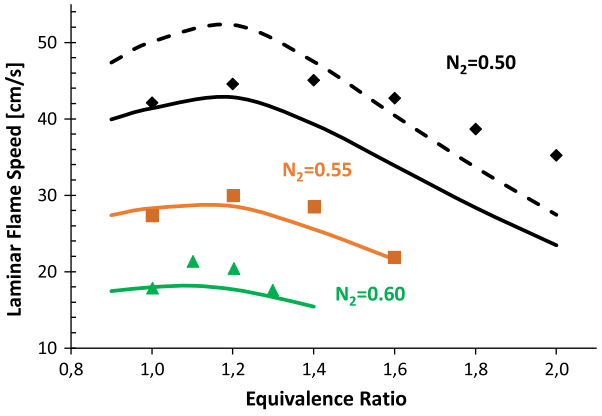

Fig. 7. Measured [105] and calculated laminar flame speeds of $H_2/Cl_2/N_2$ mixtures at 1 atm, as function of the equivalence ratio. The solid lines show calculations with the present mechanism, while the dashed line represents modeling using the value of k_9 from Leylegian et al. [105].

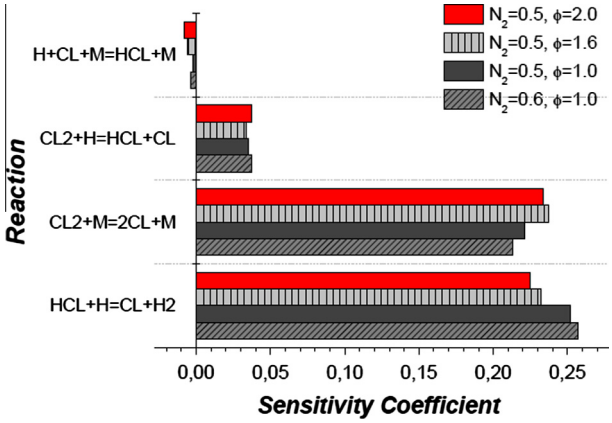

Fig. 8. Sensitivity coefficients of laminar flame speed of $H_2/Cl_2/N_2$ mixtures to rate constants at different equivalence ratios, with 50% N_2.

over the investigated equivalence ratio range, making it difficult to identify the source of the large deviations for N_2 = 0.5, ϕ > 1.4. In fact, as previously observed also by Leylegian et al. [105], a change in the rate parameters of these key reactions would simply lead to an increase/decrease in the entire flame speed curve, without strongly modifying its shape.

Leylegian and co-workers carried out a sensitivity analysis of laminar flame speed to mass diffusivity coefficients, concluding that reducing H and H_2 diffusivity and/or increasing those of Cl and Cl_2 would shift the peak in the curve to higher equivalence ratios, improving the agreement with experimental data. Since the present H_2/CO subset has already been validated over a broad range of conditions including laminar and turbulent flames [45,46], we expect the diffusion coefficients used for H and H_2 to be reliable and modifications to transport properties were not considered further in the present work.

Similarly to the predictions for H_2/Cl_2 ignition delay times, we investigated the effect of using the rate constant proposed by Leylegian et al. [105] for reaction R9b. This is shown as the dashed line in Fig. 7. The higher dissociation rate of Cl_2 enhances the predicted flame speed over full range of stoichiometries. It improves the agreement with experiment under reducing conditions but at the same time predictions become less accurate at stoichiometric and oxidizing conditions. In conclusion, given the experimental uncertainties and the observations discussed above, the agreement is considered to be satisfactory.

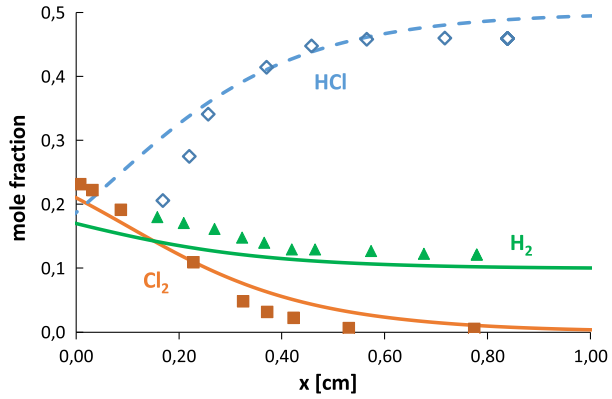

Fig. 9. Experimental [132] and calculated mole fraction profiles of H_2, Cl_2, and HCl for H_2/Cl_2/Ar flame at 42 torr.

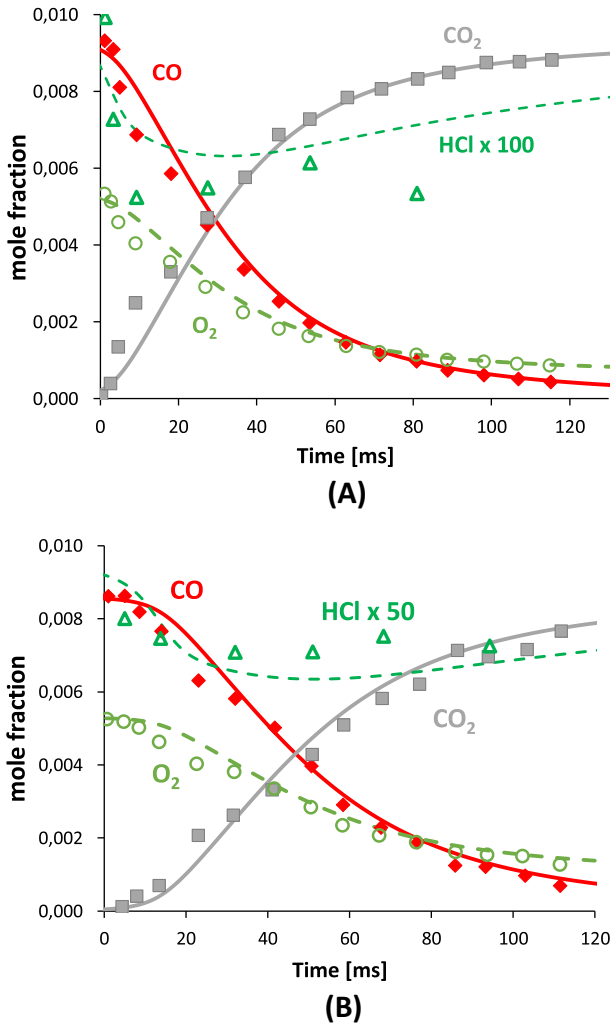

Fig. 10. Experimental (symbols) [5,6] and simulated profiles (lines) of species as function of time in stoichiometric oxidation of moist CO with 100 (A) and 190 ppm of HCl (B). Initial mixture conditions are: (A) 0.93% CO, 0.53% O_2, 0.57% H_2O, 1010 K; (B) 0.86% CO, 0.53% O_2, 0.57% H_2O, 1005 K.

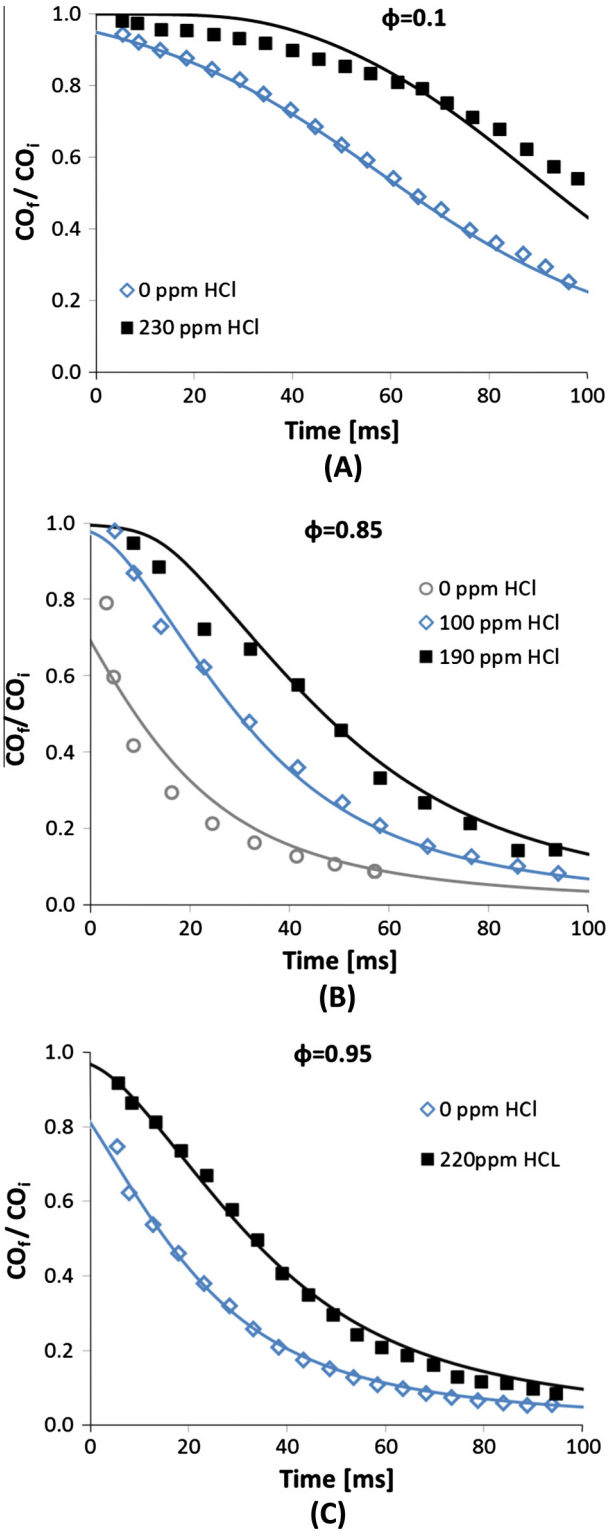

Fig. 11. Experimental (symbols) and calculated (lines) normalized CO concentration relative to the initial concentration as function of time at different amounts of HCl. (A) lean oxidation ($\phi \approx 0.1$) of moist CO 0.98% CO, 5.0% O_2, 0.6% H_2O, 1000 K with 230 ppm HCl (squares) and without HCl addition (diamonds) [28]. (B) quasi-stoichiometric ($\phi \approx 0.85$) oxidation of moist CO with 100 (diamonds) and 190 ppm (squares) of HCl [5,6]; (C) stoichiometric ($\phi \approx 0.95$) oxidation of moist CO with 220 ppm HCl (squares) and without HCl addition (diamonds) [5,6].

4.3. Flame structure of H_2/Cl_2/Ar mixtures

Vandooren et al. [132] studied the structure of a rich premixed H_2/Cl_2/Ar (35%/23%/42%) flat flame using the molecular beam sampling mass spectrometry technique (MBMS). The concentration profiles of H_2, Cl_2, HCl and Ar were measured as well as the temperature profile. Simulation results, shifted downstream of 1 mm, are compared with experimental measurements in Fig. 9, showing good agreement.

4.4. Inhibition of moist CO oxidation by HCl in flow reactors

The inhibition of $CO/H_2O/O_2$ mixture reactivity by introducing small amounts of HCl has been studied experimentally by Roesler et al. [5,8] who measured concentration profiles for CO, CO_2, O_2, HCl, as well as temperature profiles, in an atmospheric pressure flow reactor at initial temperatures of approximately 1000 K and equivalence ratios ϕ of 0.1–1.0. Roesler et al. [6] presented and discussed a detailed kinetic model for this chemistry, highlighting the importance of inhibitory reaction steps such as the chain termination reactions (R1), (R6) and (R9) and reaction cycles involving the ClCO species (R54, R60).

Simulations of data from Roesler et al. are reported in Figs. 10 and 11. The modeling predictions of Roesler et al. [6] are compared with those of the present model in the Supplementary Material. Calculations were performed assuming an adiabatic plug flow reactor. The calculated profiles have been time shifted to match 50% fuel conversion. Fig. 10 compares calculated and measured species profiles as function of time for stoichiometric mixture of moist $CO/O_2/H_2O$ with trace amounts of HCl (panel A: 100 ppm, panel B: 190 ppm). In general the model captures well the experimental data. As discussed by Roesler et al. [6], large uncertainties are associated with HCl measurements; thus, despite the slight deviations, the agreement is considered to be reasonable.

Fig. 11 compares CO conversion for lean to stoichiometric CO/O_2 for varying HCl concentration (0–230 ppm). The proposed mechanism is able to reproduce the increasing inhibiting effect obtained for increasing HCl amounts in all investigated stoichiometries.

To investigate further the inhibition effect of HCl addition to moist CO mixtures, sensitivity analyses of CO concentration to rate constants have been performed for the conditions of Fig. 11b. The normalized coefficients of the sensitive reactions are reported in Fig. 12. Panel (a) shows the reactions belonging to the H_2/CO mechanism controlling the oxidation of the investigated mixtures. As expected the formation/disappearance of CO is strictly connected to the competition between the chain branching reaction $H + O_2 \rightleftharpoons O + OH$ and the third order reaction leading to the formation of the less reactive HO_2 radical ($H + O_2 + M \rightleftharpoons HO_2 + M$). It is of interest to notice how the addition of HCl to the system leads to a large increase of the sensitivity coefficients of the H_2/CO system. This is explained on the basis of the introduction of a competing reaction channel consuming H radicals: the highly sensitive reaction R2b ($HCl + H \rightleftharpoons Cl + H_2$), whose positive sensitivity coefficient is reported in Fig. 12b. Hydrogen chloride is also consumed by the branching reaction R3 ($HCl + O \rightleftharpoons Cl + OH$) highlighted as reactivity promoter, due to its contribution to the production of reactive OH radicals. The chain termination reaction R6 ($Cl + HO_2 \rightleftharpoons HCl + O_2$), significantly contributes to a decreased reactivity, despite Cl consumption is dominated by the competing branching channel $Cl + HO_2 \rightleftharpoons OH + ClO$ (R7).

Further details of the reaction cycles involved in the inhibition process are provided by Fig. 13 showing the reaction rates (in kmol m^3 s^{-1}) over normalized time. HCl is firstly consumed by reaction with O and H radicals (R3, R2) leading to the formation of Cl radical which subsequently reacts with HO_2, forming ClO + OH via the dominating branching reaction R7 or through the termination reaction R6 ($Cl + HO_2 \rightleftharpoons HCl + O_2$). ClO is then consumed by rapid reactions with H and OH as discussed previously ((R21)–(R23)).

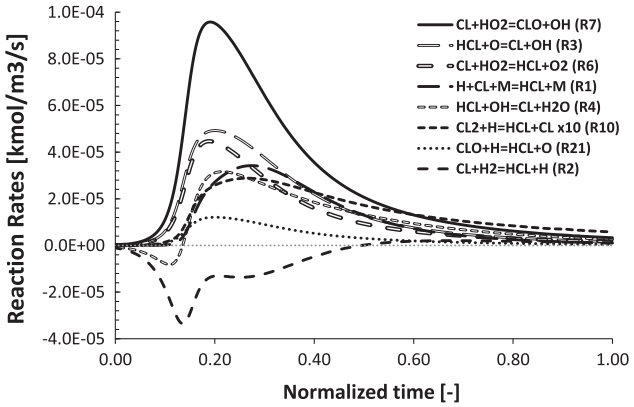

Fig. 13. Reaction rates of significant reaction steps involving HCl, 0.93% CO, 0.53% O_2, 0.57% H_2O, 1010 K, 100 ppm HCl.

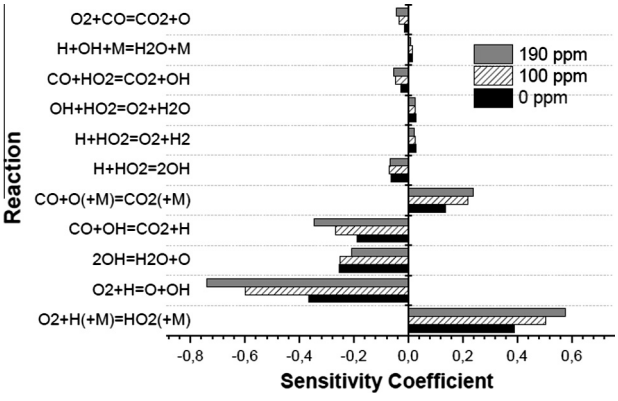

Fig. 12. Sensitivity coefficients of CO concentrations to rate constants in an atmospheric pressure flow reactor, for stoichiometric mixtures of $CO/H_2O/O_2$ and varying HCl addition quantities.

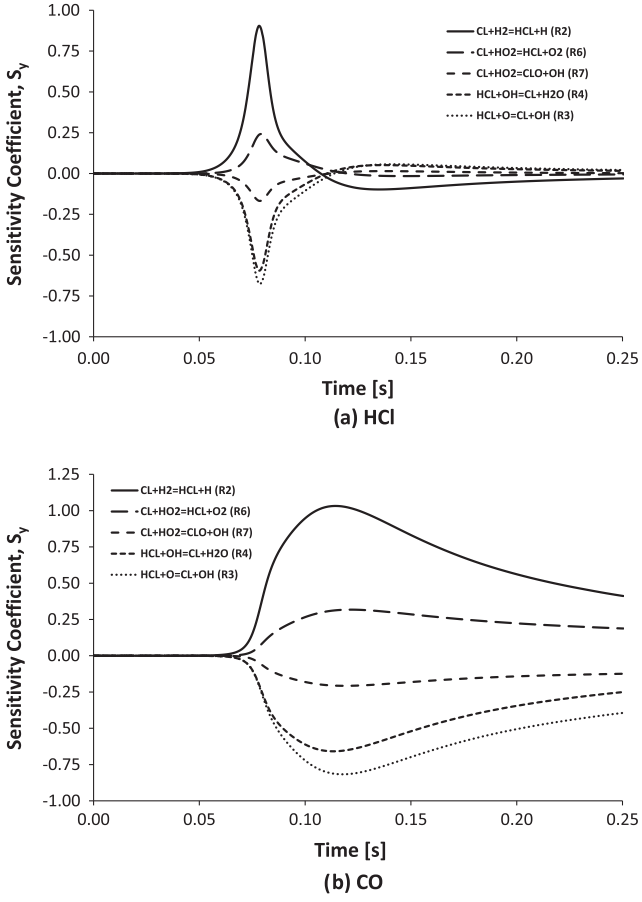

Fig. 14. Profile of largest HCl (a) and CO (b) sensitivity coefficients to rate constants for reactions discussed in this section.

As the radical pool builds up, HCl is newly produced by both termination (R1: H + Cl + M ⇌ HCl + M) and propagation steps (R10: Cl_2 + H ⇌ HCl + Cl, R22: ClO + H ⇌ HCl + O). It is also of interest to notice the inversion happening for reaction R4 (HCl + OH ⇌ Cl + H_2O), firstly contributing to chain branching (R4b) and then to HCl consumption (R4). This trend is partly due to the presence of water in the initial mixture.

In conclusion, the HCl profiles shown in Fig. 10 are explained by the reaction cycles identified by the sensitivity and the reaction rates analyses: the radical pool building up in the first stages of the oxidation consumes HCl, subtracting active radicals (H and OH mainly), thus inhibiting the system. As the Cl concentration increases, the reverse reactions become important, reducing the HCl consumption rate to zero. Similar observations were presented by Roesler et al. [5]. This is even more evident looking at the sensitivity coefficients as function of the residence time as reported in Fig. 14: the peaks in the sensitivity of HCl (panel a) to the reactions described above occur around 80 ms residence time where more than 70% of CO is consumed. After this time the sensitivity coefficients of CO largely prevail (panel b).

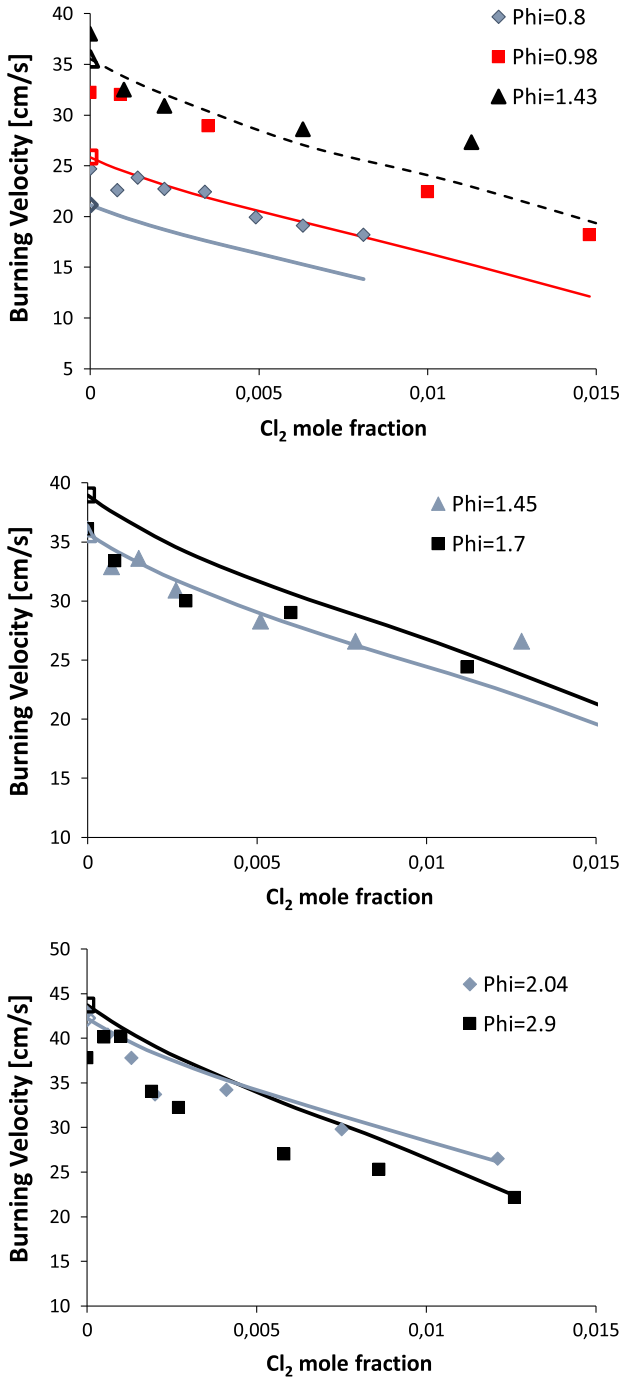

Fig. 15. Effect of Cl_2 addition on the burning velocities of CO/H_2/air at different equivalence ratios. Experimental data (symbols) [124] and calculated profiles (lines).

4.5. Chlorine inhibition of CO flames

The impact of varying amounts of Cl_2 on CO/H_2 laminar burning velocities has been investigated by Palmer and Seery [124] at an initial temperature of 298 K adopting the Bunsen cone method. The reaction mixture was prepared by blending CO/H_2 mixtures (98/2) with dry air and Cl_2. The different chlorine loadings were obtained by replacing equivalent moles of air with Cl_2. Different equivalence ratios for the CO/O_2 system were considered. It has to be noted that due to the minimal amounts of H_2 and Cl_2, the equivalence ratio defined on the basis of complete CO oxidation only slightly differs from that defined over the CO/H_2 mixture or considering the replacement of air with Cl_2.

Results for different equivalence ratios and Cl_2 loadings are reported in Fig. 15. The CO/H_2 subset [45,46] is able to reproduce well burning velocities of pure CO/air ($X_{Cl_2} = 0$; open symbols in Fig. 15). When introducing Cl_2 into the mixture, the model agrees reasonably well with the eperimental data for reducing conditions (ϕ = 1.43, 1.45, 2.04). However, for stoichiometric and lean conditions (ϕ = 0.8, 0.98), the predicted laminar burning velocities are considerably lower (5–10 cm s^{-1}) than those reported by Palmer and Seery. Similar deviations were observed with the model by Chang et al. [34] who attributed the differences partly to experimental uncertainties, including a high sensitivity to mixture impurities.

Overall, despite relatively large deviations, we believe that the kinetic mechanism presented in this study describes the inhibition of CO/H_2 flames satisfactorily, particularly in terms of the major features: increasing flame speeds for increasing equivalence ratios given a certain amount of Cl_2, decreasing flame speeds for increasing amounts of Cl_2 (see Fig. 15).

Fig. 16 presents sensitivity coefficients of laminar burning velocities to rate constants for the ϕ = 1.43 mixture reported in Fig. 14a for two different Cl_2 addition quantities ($X_{Cl_2} = 0.005$ and $X_{Cl_2} = 0.01$). Sensitivity coefficients to Cl_2/HCl specific reactions increase for increasing amounts of Cl_2. In particular, it is of

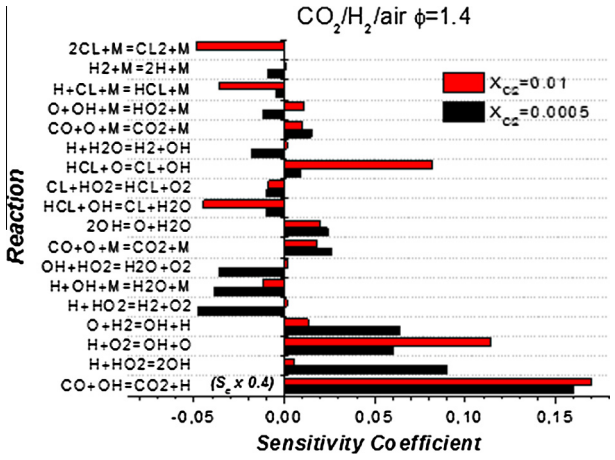

Fig. 16. Sensitivity coefficients of laminar burning velocities to rate constants for ϕ =1.43 mixtures of CO/H_2/air for two different Cl_2 addition quantities.

interest to notice the negative sensitivity to the recombination reactions (R1 and R9), together with that of reaction R4 consuming active radical OH to produce water and the less reactive Cl radical. Conversely reaction R3 producing OH is highlighted as reactivity enhancer.

5. Conclusions

The high temperature chlorine chemistry was updated and the inhibition mechanism involving HCl and Cl_2 re-evaluated. The Cl/H/O system was coupled with a H_2/CO subset to obtain a 25 species/102 reactions mechanism. The thermochemistry of chlorine species of interest was obtained using the Active Thermochemical Tables (ATcT) approach. Based on an evaluation of the rate constants available in the literature, the H_2/Cl_2/HCl/CO/O_2 mechanism was updated and validated against selected experimental data allowing a thorough analysis of the inhibition effect of chlorine and hydrogen chloride. Key reaction steps were identified; for a few of them, the need of better assessment of rate parameters was pointed out.

Modeling predictions for both shock tube ignition delay times and laminar flame speeds for the H_2/Cl_2 system were found to be very sensitive to the rate constant for the dissociation reaction $Cl_2 + M \rightleftharpoons Cl + Cl + M$. The H_2/Cl_2 shock tube and laminar flame data appear to support a value of this rate constant, which conflicts with direct measurements, and more work is required to resolve this difference. For oxygen containing mixtures, the extrapolation to high temperature for the rate constant of the $Cl + HO_2$ reaction is uncertain; in particular the branching fraction of the reaction to the competing channels $HCl + O_2$ and $Cl + HO_2$. With the present thermochemistry and rate constants, reaction cycles involving HOCl and ClCO were found not to be important under the investigated conditions.

In conclusion, the kinetic mechanism here discussed and validated represents a reliable first step towards the extension of the chemistry of chlorine species/fuel interactions to heavier molecular weights halogen compounds such as chloromethane, largely affecting combustion processes and pollutants formation.

Acknowledgments

BR was supported by the US Department of Energy, Office of Science, Office of Basic Energy Sciences, Division of Chemical Sciences, Geosciences and Biosciences under Contract No. DE-AC02-06CH11357. PG would like to acknowledge funding from the Danish Strategic Research Council.

Appendix A. Supplementary material

Supplementary data associated with this article can be found, in the online version, at http://dx.doi.org/10.1016/j.combustflame.2015.04.002.

References

[1] P. Glarborg, Proc. Combust. Inst. 31 (2007) 77–98.
[2] W. Linak, J. Wendt, Prog. Combust. Energy Sci. 19 (1993) 145–185.
[3] B. Stanmore, Combust. Flame 136 (2004) 398–427.
[4] M. Altarawneh, B. Dlugogorski, E. Kennedy, Prog. Combust. Energy Sci. 35 (2009) 245–274.
[5] J. Roesler, R. Yetter, F. Dryer, Combust. Sci. Techn. 82 (1992) 87–100.
[6] J. Roesler, R. Yetter, F. Dryer, Combust. Sci. Techn. 85 (1992) 1–22.
[7] J. Roesler, R. Yetter, F. Dryer, Combust. Sci. Techn. 101 (1994) 199–229.
[8] J. Roesler, R. Yetter, F. Dryer, Combust. Flame 100 (1995) 495.
[9] J. Roesler, R. Yetter, F. Dryer, Combust. Sci. Techn. 120 (1996) 11–37.
[10] G. Dixon-Lewis, P. Marshall, B. Ruscic, A. Burcat, E. Goos, A. Cuoci, A. Frassoldati, T. Faravelli, P. Glarborg, Combust. Flame 159 (2012) 528–540.
[11] W. Linak, J. Wendt, Combust. Sci. Technol. 115 (1996) 69–82.
[12] J. Howard, W. Kausch Jr., Prog. Energy Combust. Sci. 6 (1980) 263–276.
[13] B. Haynes, H. Jander, H. Mätzing, H. Wagner, Proc. Combust. Inst. 19 (1982) 1379–1385.
[14] W. Linak, J. Wendt, Fuel Process. Technol. 39 (1994) 173–198.
[15] B. Miller, D. Dugwell, R. Kandiyoti, Energy Fuels 17 (2003) 1382–1391.
[16] C. Senior, A. Sarofim, T. Zeng, J. Helble, R. Mamani-Paco, Fuel Process. Technol. 63 (2000) 197–213.
[17] R. Sliger, J. Kramlich, N. Marinov, Fuel Process. Technol. 65 (2000) 423–438.
[18] Y. Byun, M. Cho, W. Namkung, K. Lee, D. Koh, D. Shin, Env. Sci. Technol. 44 (2010) 1624–1629.
[19] K. Christensen, M. Stenholm, H. Livbjerg, J. Aerosol Sci. 29 (1998) 421–444.
[20] B. Jenkins, L. Baxter, T. Miles, Fuel Process. Technol. 54 (1998) 17–46.
[21] J. Werther, M. Saenger, E. Hartge, T. Ogada, Z. Siagi, Prog. Combust. Energy Sci. 26 (2000) 1–27.
[22] H. Nielsen, F. Frandsen, K. Dam-Johansen, L. Baxter, Prog. Combust. Energy Sci. 26 (2000) 283–298.
[23] J. Knudsen, P. Jensen, K. Dam-Johansen, Energy Fuels 18 (2004) 1385–1399.
[24] J. Mulholland, A. Sarofim, J. Beer, Combust. Sci. Technol. 85 (1992) 405–417.
[25] H. Wang, T. Hahn, C. Sung, C. Law, Combust. Flame 105 (1996) 291–307.
[26] C. Casias, J. McKinnon, Combust. Sci. Technol. 116 (1996) 289–315.
[27] J. Brouwer, J. Longwell, A. Sarofim, R. Barat, J. Bozzelli, Combust. Sci. Technol. 85 (1992) 87–100.
[28] X. Wei, X. Han, U. Schnell, J. Maier, H. Wörner, K. Hein, Energy Fuels 17 (2003) 1392–1398.
[29] K. Hickson, L. Keyser, J. Phys. Chem. A 109 (2005) 6887–6900.
[30] D.L. Baulch, J. Duxbury, S.J. Grant, D.C. Montague, National Standard Reference Data System, 1981.
[31] S. Senkan, Gas-Phase Combustion Chemistry, second ed., Springer-Verlag, 2000. Chapter 4: Survey of Rate Coefficients in the C/H/Cl/O System, W.C. Gardiner (Ed.).
[32] S. Karra, D. Gutman, S. Senkan, Combust. Sci. Techn. 60 (1988) 45–62.
[33] W.-P. Ho, R. Barat, J. Bozzelli, Combust. Flame 88 (1992) 265–295.
[34] W. Chang, S. Karra, S. Senkan, Combust. Flame 69 (1987) 113.
[35] B. Ruscic, R. Pinzon, M. Morton, G. von Laszewski, S. Bittner, S.G. Nijsure, K.A. Amin, M. Minkoff, A.F. Wagner, J. Phys. Chem. A 108 (2004) 9979–9997.
[36] B. Ruscic, R.E. Pinzon, G. von Laszewski, D. Kodeboyina, A. Burcat, D. Leahy, D. Montoya, A.F. Wagner, J. Phys. Conf. Ser. 16 (2005) 561–570.
[37] B. Ruscic, R.E. Pinzon, M.L. Morton, N.K. Srinivasan, M.-C. Su, J.W. Sutherland, J.V. Michael, J. Phys. Chem. A 110 (2006) 6592–6601.
[38] S. Weaver, D. Woon, B. Ruscic, B. McCall, Astrophys. J. 697 (2009) 601–609.
[39] W.R. Stevens, B. Ruscic, T. Baer, J. Phys. Chem. A 114 (2010) 13134–13145.
[40] B. Ruscic, D. Feller, K. Peterson, Theor. Chem. Acc. 133 (2014) 1415/1–12.
[41] B. Ruscic, J.V. Michael, P.C. Redfern, L.A. Curtiss, K. Raghavachari, J. Phys. Chem. A 102 (1998) 10889–10899.
[42] B. Ruscic, M. Litorja, R.L. Asher, J. Phys. Chem. A 103 (1999) 8625–8633.
[43] B. Ruscic, J. Phys. Chem. A 119 (2015).
[44] B. McBride, S. Gordon, Computer program for calculating and fitting thermodynamic functions, Tech. Rep. NASA Ref. Pub. 1271, NASA Lewis Research Center, Cleveland, Ohio, 1992.
[45] A. Frassoldati, T. Faravelli, E. Ranzi, Int. J. Hydrogen Energy 32 (2007) 3471–3485.
[46] A. Cuoci, A. Frassoldati, T. Faravelli, E. Ranzi, Int. J. Hydrogen Energy 32 (2007) 3486–3500.
[47] G. Schading, P. Roth, Combust. Flame 99 (1994) 467–474.
[48] G. Adusei, A. Fontijn, Proc. Combust. Inst. 25 (1994) 801–808.
[49] T. Xie, J. Bowman, K. Peterson, B. Ramachandran, J. Chem. Phys. 119 (2003) 9601–9608.
[50] M. Bryukov, B. Dellinger, V. Knyazev, J. Phys. Chem. A 110 (2006) 936–943.
[51] R. Atkinson, D. Baulch, R. Cox, J. Crowley, R. Hampson Jr., R. Hynes, M. Jenkin, M. Rossi, J. Troe, Atmos. Chem. Phys. 7 (2007) 981–1191.
[52] P. Wine, J. Nicovich, A. Ravishankara, J. Phys. Chem. 89 (1985) 3914.
[53] M. Bryukov, V. Knyazev, S. Lomnicki, C. McFerrin, B. Dellinger, J. Phys. Chem. A 108 (2004) 10464–10472.
[54] Z. Xu, M. Lin, J. Phys. Chem. A 113 (2009) 8811–8817.
[55] L. Wang, J. Liu, Z. Li, X. Huang, C. Sun, J. Phys. Chem. A 107 (2003) 4921–4928.
[56] S. Wategaonkar, D. Setser, J. Chem. Phys. 90 (1989) 6223–6233.
[57] R. Zhu, M. Lin, Comput. Theor. Chem. 965 (2011) 328–339.
[58] R. Zhu, M. Lin, J. Chem. Phys. 119 (2003) 2075–2082.
[59] S. Wategaonkar, D. Setser, J. Chem. Phys. 90 (1989) 251–264.
[60] R. Zhu, M. Lin, J. Phys. Chem. A 106 (2002) 8386–8390.
[61] Z. Xu, R. Zhu, M. Lin, J. Phys. Chem. A 107 (2003) 1040–1049.
[62] R. Zhu, M. Lin, J. Chem. Phys. 118 (2003) 8645–8655.
[63] , J. Phys. Chem. 96 (1992) 2582–2588.
[64] R. Atkinson, D. Baulch, R. Cox, R. Hampson Jr., J. Kerr, M. Rossi, J. Troe, J. Phys. Chem. Ref. Data 26 (1997) 521–1009.
[65] Y. Tian, W.-M. Wei, Z.-M. Tian, H.-Y. Yang, T.-J. He, F.-C. Liu, D.-M. Chen, J. Phys. Chem. A 110 (2006) 11145–11150.
[66] R. Timonen, E. Ratajczak, D. Gutman, J. Phys. Chem. 92 (1988) 651–655.
[67] F. Louis, C. Gonzales, J.-P. Sawersyn, J. Phys. Chem. A 107 (2003) 9931–9936.
[68] Z. Qu, F. Dong, Q. Zhang, F. Kong, Chem. Phys. Lett. 386 (2004) 384–389.
[69] Q. Li, Q. Luo, J. Phys. Chem. A 107 (2003) 10435–10440.
[70] J. Francisco, J. Chem. Phys. 96 (1992) 7597–7602.
[71] R. Barat, J. Longwell, A. Sarofim, J. Bozzelli, Combust. Sci. Technol. 74 (1990) 361.
[72] T. Clarke, M. Clyne, D. Stedman, Trans. Faraday Soc. 62 (1966) 3354–3365.
[73] E. Fishburne, J. Chem. Phys. 45 (1966) 4053–4056.
[74] T. Jacobs, N. Cohen, R. Giedt, J. Chem. Phys. 46 (1967) 1958–1968.

[75] D. Seery, C. Bowman, J. Chem. Phys. 48 (1968) 4314.
[76] R. Giedt, T. Jacobs, J. Chem. Phys. 55 (1971) 4144.
[77] W. Breshears, P. Bird, J. Chem. Phys. 56 (1972) 5347.
[78] P. Ambidge, J. Bradley, D. Whytock, J. Chem. Soc. Faraday Trans. 1 72 (1976) 2143.
[79] J. Miller, R. Gordon, J. Chem. Phys. 75 (1981) 5305.
[80] D. Kita, D. Stedman, J. Chem. Soc. Faraday Trans. 2 78 (1982) 1249.
[81] G. Adusei, A. Fontijn, J. Phys. Chem. 97 (1993) 1409.
[82] A. Westenberg, N. deHaas, J. Chem. Phys. 48 (1968) 4405.
[83] J. Lee, J. Michael, W. Payne, L. Stief, D. Whytock, J. Chem. Soc. Faraday Trans. 1 73 (1977) 1530.
[84] F. Su, J. Calvert, C. Lindley, W. Uselman, J. Shaw, J. Chem. Phys. 83 (1979) 912.
[85] S. Kumaran, K. Lim, J. Michael, J. Chem. Phys. 101 (1994). pp. 9487-9408.
[86] T. Allison, G. Lynch, D. Truhlar, M. Gordon, J. Phys. Chem. 100 (1996) 13575–13587.
[87] U. Manthe, G. Capecchi, H.-J. Werner, Phys. Chem. Chem. Phys. 6 (2004) 5026–5030.
[88] H. Wagner, U. Welzbacher, R. Zellner, Ber. Bunsenges. Phys. Chem. 80 (1976) 902.
[89] P. Bemand, M. Clyne, J. Chem. Soc. Faraday Trans. 2 73 (1977) 394.
[90] F. Berho, M.-T. Rayez, R. Lesclaux, J. Phys. Chem. A 103 (1999) 5501–5509.
[91] A. Lloyd, Int. J. Chem. Kinet. 2 (1971) 39.
[92] H. Hiraoka, R. Hardwick, J. Chem. Phys. 36 (1963) 1715.
[93] R. Diesen, W. Felmlee, J. Chem. Phys. 39 (1963) 2115.
[94] T. Jacobs, R. Giedt, J. Chem. Phys. 39 (1963) 749.
[95] M. van Thiel, D. Seery, D. Britton, J. Phys. Chem. 69 (1965) 834.
[96] R. Carabetta, H. Palmer, J. Chem. Phys. 46 (1967) 1333.
[97] J. Blauer, H. McMath, F. Jaye, J. Phys. Chem. 73 (1969) 2683.
[98] R. Santoro, G. Diebold, G. Goldsmith, J. Chem. Phys. 67 (1977) 881.
[99] L. Bader, E. Ogryzlo, Nature 201 (1964) 491.
[100] E. Hutton, M. Wright, Trans. Faraday Soc. 61 (1965) 78.
[101] M. Clyne, D. Stedman, Disc. Faraday Soc. 44 (1967) 276.
[102] M. Clyne, D. Stedman, Trans. Faraday Soc. 64 (1968) 2698.
[103] R. Widman, B. DeGraaf, J. Phys. Chem. 77 (1973) 1325.
[104] P. Nording, D. Rosner, JCS Faraday I 26 (2000) 283–298.
[105] J. Leylegian, H. Sun, C. Law, Combust. Flame 143 (2005) 199–210.
[106] K. Mahmoud, J. Kim, A. Fontijn, J. Phys. Chem. 94 (1990) 2994–2998.
[107] C.-C. Hsiao, Y.-P. Lee, N. Wang, J. Wang, M. Lin, J. Phys. Chem. A 106 (2002) 10231–10237.
[108] W. Hack, G. Mex, H. Wagner, Ber. Bunsenges. Phys. Chem. 81 (1977) 677.
[109] D. Husain, J. Plane, C. Xiang, J. Chem. Soc. Faraday Trans. 2 80 (1984) 713–728.
[110] A. Ravishankara, P. Wine, J. Wells, R. Thompson, Int. J. Chem. Kinet. 17 (1985) 1281.
[111] J. Michael, D. Whytock, J. Lee, W. Payne, L. Stief, J. Chem. Phys. 67 (1977) 3533–3536.
[112] L. Keyser, J. Phys. Chem. 84 (1980) 11.
[113] Y.-P. Lee, C. Howard, J. Chem. Phys. 77 (1982) 756.
[114] V. Riffault, Y. Bedjanian, G.L. Bras, Int. J. Chem. Kinet. 33 (2001) 317–327.
[115] A. Gavriliv, V. Kochubei, F. Moin, Kinet. Cat. 16 (1975) 666.
[116] C. Ennis, J. Birks, J. Phys. Chem. 92 (1988) 1119.
[117] R. Vogt, R. Schindler, Ber. Bunsenges. Phys. Chem. 97 (1993) 819–829.
[118] R. Schindler, J. Dethlefs, M. Schmidt, Ber. Bunsenges. Phys. Chem. 7 (1996) 1242–1249.
[119] J. Lipson, M. Elrod, T. Beiderhase, L. Molina, M. Molina, J. Chem. Soc. Faraday Trans. 93 (1997) 2665.
[120] J. Lipson, T. Beiderhase, L. Molina, M. Molina, M. Olzmann, J. Phys. Chem. A 103 (1999) 6540.
[121] Y. Bedjanian, V. Riffault, G.L. Bras, Int. J. Chem. Kinet. 33 (2001) 587–599.
[122] M. Finkbeiner, J. Crowley, O. Horie, R. Muller, G. Moortgat, P. Crutzen, J. Phys. Chem. 99 (1995) 16264–16275.
[123] K. Hickson, L. Keyser, S. Sander, J. Phys. Chem. A 111 (2007) 8126–8138.
[124] H. Palmer, D. Seery, Combust. Flame 4 (1960) 213–221.
[125] M. Clyne, R. Watson, J. Chem. Soc., Faraday Trans. 70 (1974) 2250.
[126] J. Nicovich, K. Kreutter, P. Wine, J. Chem. Phys. 92 (1990) 3539.
[127] A. Hewitt, K. Brahan, G. Boone, S. Hewitt, Int. J. Chem. Kinet. 28 (1996) 763–771.
[128] R. Atkinson, D. Baulch, R. Cox, J. Crowley, R. Hampson, R. Hynes, M. Jenkin, M. Rossi, J. Troe, Atmos. Chem. Phys. 4 (2004) 1461–1738.
[129] C. Park, J. Phys. Chem. 81 (1977) 499.
[130] A. Umland, J. Electrochem. Soc. 101 (1954) 626–631.
[131] P. Ashmore, Proc. Combust. Inst. 5 (1955) 700–705.
[132] J. Vandooren, R. Fristrom, P.V. Tiggelen, Bull. Soc. Chim. Belg. 10 (1992) 901–907.
[133] A. Lifshitz, P. Schechner, Int. J. Chem. Kinet. 7 (1975) 125–142.
[134] A. Cuoci, A. Frassoldati, T. Faravelli, E. Ranzi, OpenSMOKE: numerical modeling of reacting systems with detailed kinetic mechanisms, XXXIV meeting of the Italian Section of the Combustion Institute, 2011.
[135] A. Cuoci, A. Frassoldati, E. Ranzi, T. Faravelli, OpenSMOKE++: an object oriented framework for the numerical modeling of reactive systems with detailed kinetic mechanisms, Comput. Phys. Commun (2015).